Direct Observation of Carbon Particle SCWO Progress by X-ray Radiography

Makoto Fujie
Joint Research Center for Supercritical Fluids, Japan Chemical Innovation Institute, Nigatake, Sendai 983-8551, Japan

Hisao Ohmura
Power & Industrial Systems Research & Development Center, Toshiba Corporation, 4-1 Ukishima-cho, Kawasaki-ku, Kawasaki 210-0862, Japan

Chikara Konagai and Koichi Nittoh
Power & Industrial Systems Research & Development Center, Toshiba Corporation, 8 Shinsugita-cho, Isogo-ku, Yokohama 235-8523, Japan

Masakazu Sugiyama
Dept. of Electronic Engineering, School of Engineering, The University of Tokyo, Tokyo 113-8656, Japan

Kazuhiko Maeda and Seiichiro Koda
Dept. of Chemistry, Faculty of Science and Technology, Sophia University, Tokyo 102-8554, Japan

DOI 10.1002/aic.10524
Published online June 29, 2005 in Wiley InterScience (www.interscience.wiley.com).

Keywords: supercritical water, supercritical water oxidation, SCWO, graphite, X-ray radiography

We previously succeeded in directly observing the reaction progress of carbon particles under supercritical water oxidation (SCWO) conditions using shadowgraph[1,2] and/or the Schlieren photographic method,[3] where a reaction cell equipped with sapphire windows for light transmission was used. However, it is a formidable challenge to use sapphire windows for monitoring SCWO progress more generally at high temperature and high pressure. At the same time, the previous visualization methods do not allow one to observe the reaction progress inside of the particles, although such latent reactions were suspected in the case of a graphite particle.[2] Thus we have tried to adopt X-ray radiography to follow the reaction progress in a reaction apparatus without any optical windows and also in the particle itself. In the present work, we will show the SCWO progress of a graphite particle to demonstrate the usefulness of X-ray radiography. The complete time evolution has been successfully followed, thus demonstrating the future potential of X-ray radiography.

Correspondence concerning this article should be addressed to S. Koda at s-koda@sophia.ac.jp.

Experimental

Reaction system and procedure

The reaction proceeded in a vertical tubular reactor of Inconel® 625 (ID: 11.0 mm; OD: 19.0 mm; height: ~1.5 m), which was covered by heating tapes. The pressurized water or aqueous H_2O_2 with a syringe pump (ISCO Model 100DM) was introduced through the preheater section to the bottom of the tube reactor, flew upward, and exited through the heat exchanger and the back pressure regulator to control the reactor pressure. The concentration of aqueous H_2O_2 was chosen to produce the desired concentration of O_2–water mixture, confirming that H_2O_2 was stoichiometrically decomposed in the preheater to produce O_2.[4] From a height of 15 to 45 cm from the inlet of the water flow, the outer diameter of the Inconel® tube was 14.2 mm, from which the heating tape was stripped, and the tube was covered by a thin aluminum film, where the X-ray was introduced perpendicular to the reactor tube. The

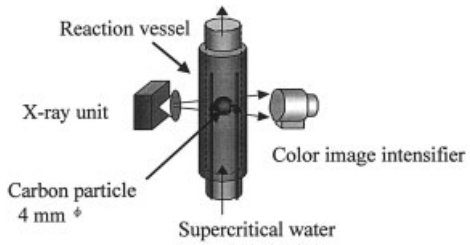

Figure 1. Setup for X-ray radiography monitoring SCWO of a carbon particle.

temperature inside of the reactor tube was monitored with sealed thermocouples at 8 and 70 cm height from the inlet of the water flow. The temperatures at the two monitoring thermocouples were controlled within ±1°C of the desired temperature. The transmitted X-ray was detected by a color-image intensifier.

The arrangement of the sample and the X-ray system is illustrated in Figure 1. The sample for the present work was a commercially obtained synthetic graphite particle (diameter: 4 mm; density: 1.72 g cm^{-3}; ash content: 200 ppm). The sample was positioned on a spiral of Pt wire, supported between two thin supporting rods inside of the tube reactor. In the experimental procedure, after the sample was located at the appropriate position, water was introduced. After the total system was stabilized at the desired conditions (typically 500°C and 30 MPa), water was replaced by aqueous H_2O_2, if necessary.

The adopted X-ray radiographic system is a newly devised system with a multicolor scintillator-based, highly sensitive, wide-dynamic-range, and long-life X-ray image intensifier. Details of the X-ray imaging system were described previously.[5,6] Briefly, an X-ray tube, of 150 kV and 3 mA, was adopted. The effective energy used was 60 keV at the tube reactor, and the observation range by the X-ray beams spanned about 6 × 8 cm. The signals were usually integrated for 8 s.

To check the sensitivity and the linearity between the obtained signal intensity and the density of the sample in advance, X-ray images were obtained under ambient conditions for a cylindrical step-gauge made of a series of graphite particles of different diameters, which was placed under a location similar to that adopted for the carbon SCWO measurements.

Results

Linearity of the experimental brightness against the density or diameter of the sample

The X-ray intensity through the sample in the present system is explained as follows. The X-ray transmits through the following three different regions: carbon, water, and the surrounding wall (which consisted primarily of Inconel® 625). The individual materials are characterized by the following parameters: linear absorption coefficient μ, density ρ, and depth d. The individual materials are identified by the suffixes c, w, and m for carbon, water, and the wall material, respectively. Eventually, however, d_w is taken as the inner tube diameter.

When the carbon sample is on the X-ray transmission line, the detected transmitted X-ray intensity is

$$I_{obs} = I_0 \exp[-\mu_m \rho_m d_m - \mu_w \rho_w (d_w - d_c) - \mu_c \rho_c d_c] \quad (1)$$

where I_0 is the intensity of the X-ray at the outer surface of the tube reactor. On the other hand, when the sample is absent, the observed intensity should be

$$I'_{obs} = I_0 \exp(-\mu_m \rho_m d_m - \mu_w \rho_w d_w) \quad (2)$$

Thus the difference signal intensity, obtained as the difference between the presence and absence of the sample, is

$$\begin{aligned}\text{Difference signal intensity} &= I'_{obs} - I_{obs} = I_0 \exp(-\mu_m \rho_m d_m \\ &- \mu_w \rho_w d_w) - I_0 \exp\{-\mu_m \rho_m d_m - \mu_w \rho_w (d_w - d_c) - \mu_c \rho_c d_c\} \\ &= I_0 \exp(-\mu_m \rho_m d_m - \mu_w \rho_w d_w)[1 - \exp\{-(\mu_c \rho_c - \mu_w \rho_w) d_c\}] \end{aligned} \quad (3)$$

The difference signal intensity was measured as the brightness on a cathode-ray tube by a signal-processing procedure. When the value $(\mu_c \rho_c - \mu_w \rho_w) d_c$ is small, the exponential term can be expanded to the first order, and the following relationship is obtained

$$\begin{aligned}\text{Brightness} \propto \text{difference signal intensity} \\ = \{I_0 \exp(-\mu_m \rho_m d_m - \mu_w \rho_w d_w)\}(\mu_c \rho_c - \mu_w \rho_w) d_c \propto d_c \end{aligned} \quad (4)$$

Thus, the brightness is proportional to the value of d_c when the diameter of the carbon particle changes without any change of the carbon particle density ρ_c. Here it is assumed that the value of $[I_0 \exp(-\mu_m \rho_m d_m - \mu_w \rho_w d_w)](\mu_c \rho_c - \mu_w \rho_w)$ is kept constant, as usually experimentally realized. Otherwise, when d_c is kept constant and the density of the carbon particle ρ_c is changed, the difference signal intensity should be linearly dependent on the change of ρ_c, particularly when the brightness is visualized as the difference from the background water

$$\text{Brightness} \propto (\mu_c \rho_c) d_c \propto \rho_c \quad (5)$$

Taking into account that μ for elemental carbon and water is 0.175 and 0.206 $cm^2\ g^{-1}$,[7] respectively, and that the density of the graphite particle and the water at the critical point is 1.72 and 0.32 g cm^{-3},[8] respectively, the value of $(\mu_c \rho_c - \mu_w \rho_w) d_c$ is small enough to allow for the first-order approximation of the exponential term expansion. For example, when d_c is 0.4 cm, the value is <0.1.

Figure 2 shows: the shape of the cylindrical step-gauge used for the calibration (top panel), the brightness image of the gauge (middle panel), and the relationship of the brightness at the central axis and the corresponding diameter of the gauge (bottom panel). The integration time for the imaging was 8 s. It is demonstrated that the diameter of the gauge can be measured from the brightness image (middle panel) itself, and also as the brightness at the axis according to Eq. 4. The change of the diameter d_c by <0.02 cm can be detected from the brightness change. Under the adopted conditions of room temperature and 1 atm, the density of water is greater than that under the supercritical conditions. Thus, the difference between the carbon and water for the X-ray absorption is smaller in Figure 2 than that for the critical conditions, which implies a higher sensitivity under the SCWO experimental conditions than the present ambient conditions.

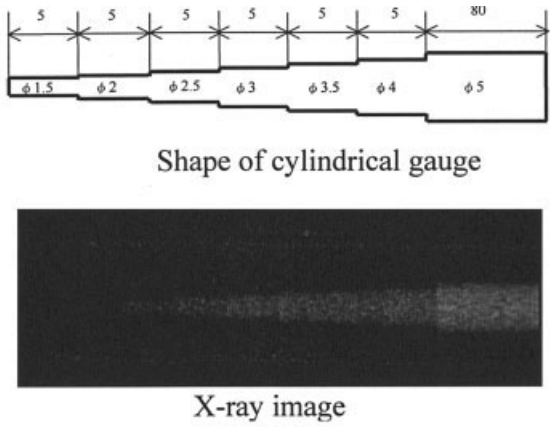

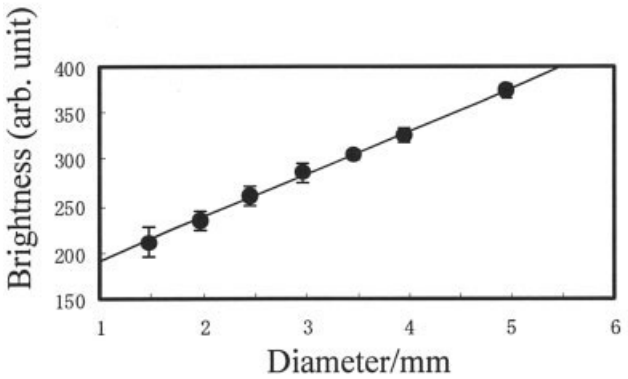

Figure 2. Calibration of the brightness of X-ray image using a tapered carbon step-gauge in ambient water in the Inconel® reactor.

The shape of the cylindrical gauge, the brightness image of the gauge, and the relationship of the brightness at the central axis and the corresponding diameters of the gauge are shown from top to bottom.

Analysis of the time evolution and phenomenological rate constants

Figure 3 shows the brightness images of a graphite particle along with the reaction time at the temperature of 773 K and 30 MPa in the presence of 3.6 wt % O_2. The images schematically show that the particle size remains almost constant until very close to the end. Figure 4 plots the observed diameter for the vertical and horizontal directions; and Figure 5, the brightness at the sample center. The fact that the brightness decreases together with relatively small change of diameter means that the inside density of the particle changes almost uniformly. From the linear density change along the time, the reaction rate of carbon consumption for a unit initial outer surface area S_0 is estimated to be 5.8×10^{-5} kg m^{-2} s^{-1}. The reaction apparently obeys a zero-order kinetics on the carbon density. This reaction rate implies only a small temperature increase in the carbon particle (a rough estimation from the balance between the heat evolution arising from the reaction and the heat loss to the bulk flow indicates the temperature rise of around 10°C), and also that the overall reaction is not limited by the O_2 mass transfer from the bulk flow to the particle surface according to the previously developed argument.[2] Our previous study using shadowgraph technology on another graphite particle, at 773 K and 30 MPa with 10 wt % O_2, showed the rate of 7.2×10^{-5} kg m^{-2} s^{-1} after a long induction time. The apparent phenomena and the rate constants are slightly different between the

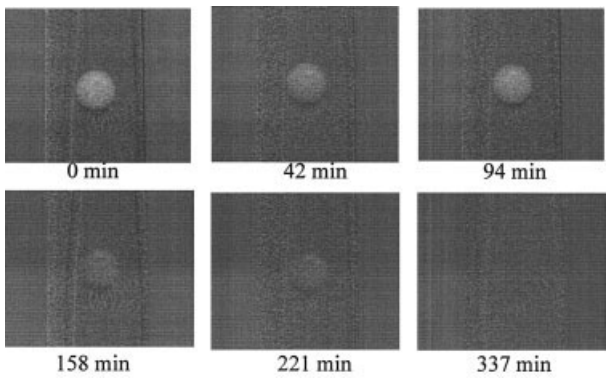

Figure 3. Image of a graphite particle during the SCWO progress at 773 K and 30 MPa, with 3.6 wt % O_2 containing water.

The flow rate of the fluid was 2 mL min^{-1} when being measured at room temperature and 1 atm.

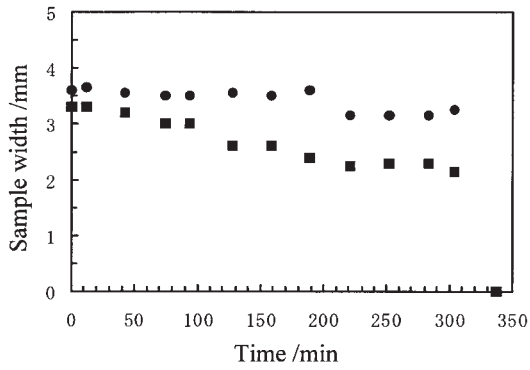

Figure 4. Time dependency of the horizontal and vertical diameter during the SCWO progress of the graphite particle.

Reaction conditions are the same for those described in the caption of Figure 3. Circle keys: horizontal diameter; square keys: vertical diameter.

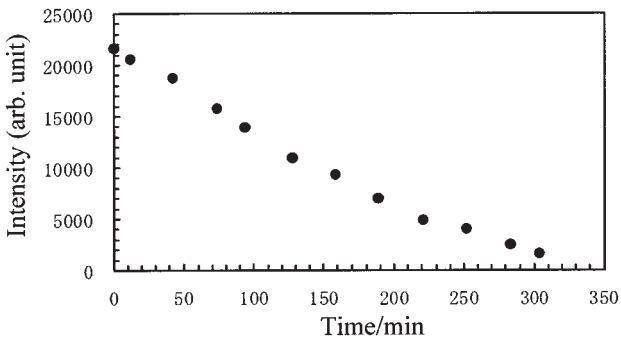

Figure 5. Time dependency of the brightness at the central region of the carbon particle.

Reaction conditions are the same for those described in the caption of Figure 3.

previous and the present experiments, probably because of the different properties of the graphite used.

Because the properties of the present graphite, such as porosity and pore size distribution, have not as yet been thoroughly investigated, any reliable estimation of the Thiele modulus is difficult. However, based on the general structure of the synthetic graphite and the present experimental reaction rate, our tentative estimation suggests that the Thiele modulus is smaller than unity, and thus the effectiveness factor is >0.7. This relatively large effectiveness factor implies that the oxidation reaction proceeds almost uniformly inside of the particle, and thus the apparent decrease of the density without noticeable change of the particle size may be understandable.

The present technology clearly demonstrated two important points: (1) the progress of the reaction can be observed even in a closed vessel without any optical windows; (2) even when any shape change is not observed by visualization, sometimes the reaction is proceeding inside of the graphite particle.

Relevance of X-ray radiography and its future applications

Important facts to be noted are: first, we have succeeded in observing the complete progress of SCWO of a graphite particle without using any optical windows. Second, the shape was maintained for a long time while the reaction was proceeding inside of the particle to decrease the density.

Apart from analysis of the carbon SCWO process, important phenomena such as salt deposition on the reactor wall and surface corrosion may also become tractable by means of the present technology in the future.

Conclusion

A visualization system using X-ray radiography was successfully applied to the observation of SCWO progress of a graphite particle in an Inconel® 625 tube reactor. It was found that the graphite particle reacted inside of the particle with only a negligible change in outer shape. This finding is novel and also demonstrates the very high potential of the present highly sensitive X-ray radiography system for observing the latent reaction progress from outside.

Acknowledgments

The present study was supported in part by a grant provided by the New Energy and Industrial Technology Development Organization [NEDO, under the auspices of Japan Chemical Innovation Institute (JCII)] based on the project "Research & Development of Environmentally Friendly Technology Using SCF" of the Industrial Science Technology Frontier Program [Ministry of Economy, Trade and Industry (METI), Japan], which is greatly appreciated.

Literature Cited

1. Sugiyama M, Ohmura H, Kataoka M, Kobayashi T, Koda S. Shadowgraph observation of supercritical water oxidation progress of a carbon particle. *Ind Eng Chem Res.* 2002;41:3044-3048.
2. Sugiyama M, Kataoka M, Ohmura H, Fujiwara H, Koda S. Oxidation of carbon particles in supercritical water: Rate and mechanism. *Ind Eng Chem Res*. 2004;43:690-699.
3. Sugiyama M, Tagawa S, Ohmura H, Koda S. Supercritical water oxidation of a carbon particle by Schlieren photography. *AIChE J*. 2004;50:2082-2089.
4. Croiset E, Rice SF, Hanush RG. Hydrogen peroxide decomposition on supercritical water. *AIChE J*. 1997;43:2343-2352.
5. Nittoh K, Oyaizu E, Sakurai T, Yoshida T, Mochiki K. Extension of dynamic range in X-ray radiography using multi-color scintillation detector. *Nucl Instrum Methods Phys Res A*. 2003;501:615-622.
6. Nittoh K, Konagai C, Noji T. Development of multi-color scintillator based X-ray image intensifier. *Nucl Instrum Methods Phys Res A*. 2004;535:686-691.
7. Henke BL, Gullikson EM, Davis JC. X-ray interactions: Photoabsorption, scattering, transmission, and reflection at E = 50–30,000 eV, Z = 1–92. *Atom Data Nucl Data*. 1993;54:181-342.
8. Haar L, Gallagher JS, Kell GS. *NBS/NRC Steam Tables*. Washington, DC: Hemisphere; 1984.

Manuscript received Dec. 7, 2004, and revision received Feb. 6, 2005.